Hindawi Publishing Corporation
Journal of Materials
Volume 2015, Article ID 652645, 5 pages
http://dx.doi.org/10.1155/2015/652645

Research Article

Solution-Processed rGO/AgNPs/rGO Sandwich Structure as a Hole Extraction Layer for Polymer Solar Cells

Quang Trung Tran,[1] Hoang Thi Thu,[1] Vinh Son Tran,[1] Tran Viet Cuong,[1] and Chang-Hee Hong[2]

[1]*Department of Solid State Physics, Faculty of Physics, University of Science, Vietnam National University-Ho Chi Minh City (VNU-HCM), 227 Nguyen Van Cu, Ward 4, District 5, Ho Chi Minh City, Vietnam*
[2]*LED Agri-Bio Fusion Technology Research Center, School of Semiconductor and Chemical Engineering, Chonbuk National University, Jeonju 561-756, Republic of Korea*

Correspondence should be addressed to Tran Viet Cuong; tvcuong@hcmus.edu.vn and Chang-Hee Hong; chhong@jbnu.ac.kr

Received 23 December 2014; Accepted 27 May 2015

Academic Editor: Carmen Alvarez-Lorenzo

We found that inserting silver nanoparticles (AgNPs) between two layers of reduced grapheme oxide (rGO) has an effect on tailoring the work function of rGO. The utilization of rGO/AgNPs/rGO sandwich structure as the hole extraction layer in polymer solar cells is demonstrated. Solution-processable fabrication of this sandwich structure at the ITO/active layer interface facilitates the extraction of hole from active layer into ITO anode because of lowering the barrier level alignment at the interface. It results in an improvement of the short circuit current density and the overall photovoltaic performance.

1. Introduction

For high performance polymer solar cells (PSCs), the interfaces of the cathode and the anode with polymers play critical roles in regulating the charge separation and charge collection and hence the overall device performance. The energy barriers between the active layer and the electrodes can be effectively reduced by using electron/hole extraction layers at the cathode/anode. Therefore, fabrication of a suitable hole extraction layer (HEL) between the anode and the active layer as well as an electron extraction layer (EEL) between the cathode and the active layer is key technology for enhancement of the PSCs device performance and lifetime. Recently, solution-based processes graphene oxide (GO) has been considered as an efficient hole transport layer for high performance organic solar cells [1, 2]. Although, GO has many advantages over organic-based HEL, one drawback of the GO is its insulating nature which leads to an increased series resistance with a concomitant decrease in fill factor (FF) and power conversion efficiency (PCE) of the resulting device [3]. An attempt to fabricate GO-based platform with higher electrical conductivity while being able to tune its work function well matching with ITO is requisite for the design and development of the GO-based HEL for high performance PSCs. Several methods to enhance the electrical property have been reported such as hybridization of GO with AgNPs, gold nanoparticles, and chemical and/or thermal reduction [4–6]. It should be noted that these approaches not only promise to improve electrical conductivity but also lead to a change in the work function of the GO films. For PSCs applications, investigation of the effect of work function on the solar cells performance is still limited up to date. In this study, a sandwich structure of rGO/AgNPs/rGO is fabricated as HEL for PSCs using solution processes. For comparison, PSCs based on chemically reduced GO (CRG) with hydrazine were also fabricated under identical conditions to elucidate the work function effect on the device performances.

2. Experimental Methods

Firstly, AgNPs solution was synthesized by the polyol method. A mixture of 0.66 g of poly(vinylpyrrolidone) (PVP)

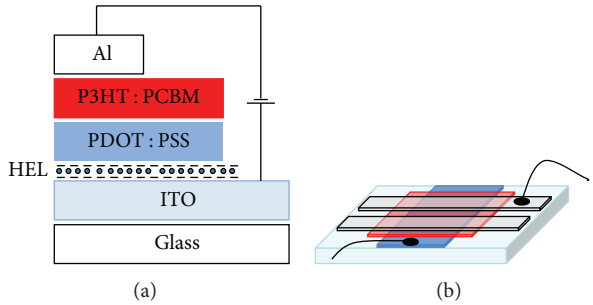

Figure 1: A schematic diagram illustrating rGO/AgNPs/rGO HEL (a) and electrode pad structures (b) of polymer solar cells.

and 20 mL of ethylene glycol (EG) was heated until thermally stabilized at 170°C in a flask, followed by adding 0.055 g of silver chloride (AgCl) to form Ag seeds. After 3 min, 0.066 g of silver nitrate ($AgNO_3$) as Ag precursor was slowly added, and the flask was further heated for 40 min to ensure the particle growth was complete. The molar ratios of [PVP]/[$AgNO_3$] and [AgCl]/[$AgNO_3$] were selected to be 15 and 1, respectively. The final product was expected to produce a large amount of PVP-coated NPs concomitant with a small amount of Ag nanowires (AgNWs). Thus, it is necessary to separate the AgNPs from the AgNWs. After allowing the solution to cool overnight, it was divided into two portions, the top portion consisting primarily of NPs aggregates and the sediment portion containing both self-assembled NWs and NPs aggregates. The solutions were centrifuged at 2000 rpm for 30 min to isolate the NPs, which remained in the sediment. The AgNPs were transferred to water by first washing with acetone to remove the excess PVP and EG, centrifugation at 5000 rpm for 5 min, and redispersing of the residue in water. This process was repeated three times to achieve final AgNPs solution. Secondly, rGO/AgNPs/rGO HEL was prepared as follows: 1 mL of synthesized GO dispersion (0.025 mg/mL) was spray-coated onto the preheated ITO-coated glass substrate at 400°C [7], the temperature was brought down to 150°C in order to spray 2 mL of AgNPs solution, and again the temperature was raised to 400°C for spraying 1 mL GO dispersion to form the sandwich structure as shown in Figure 1. It should be noted that the GO dispersion was slightly reduced to form thermally reduced graphene oxide (rGO) at 400°C of spray-coated temperature. For comparison, the GO dispersion was chemically reduced with excess hydrazine monohydrate at room temperature to form CRG which herein was used instead of HEL [8]. Subsequently, PDOT : PSS (Bayer) was diluted 1 : 1 with distilled water, filtered through 0.45 μm filter, and spin-coated at 8000 rpm. The PDOT : PSS layers were dried for 10 min at 175°C under ambient temperature in argon filled glove box with humidity level lower than 0.5 ppm. Then, poly(3-hexylthiophene) (P3HT-Merck) and (6,6)-phenyl C_{61}-butyric acid methylester (PCBM-American Dye Source), at 1 : 1 weight ratio, were both dissolved in dichlorobenzene and kept stirring at 60°C overnight. The prepared solution was spin-coated at 2000 rpm for 20 s and annealed at 140°C for 45 min. Finally a 200 nm thick Al electrode in the form of a stripe pattern was deposited using shadow mask and electron beam deposition. The cross-sectional and top-view device structures were illustrated in Figure 1. To verify the structures of samples, X-ray diffraction (XRD), Philips PW 3710, was carried out in the 2θ mode. Scanning electron microscope (SEM, Hitachi S-4200) was used to examine the morphology of the films; UV-Vis spectrophotometer (HP-8453) was employed to analyze the optical property materials in the wavelength range from 200 nm to 1100 nm. To measure the work function of prepared materials, UPS was performed on a PHI 5000 versa probe with He I (21.2 eV) source. The current density-voltage (J-V) curves were measured under ambient air using a Keithley 2400 source measurement unit. The photocurrent was measured under AM1.5G 100 mW/cm^{-2} illumination from an Oriel 150 W solar simulator.

3. Results and Discussion

Figure 2(a) shows the SEM image of as-prepared rGO/AgNPs/rGO HEL. As can be seen, the AgNPs are randomly arranged and fully covered by rGO. The AgNPs size is irregular and their diameter varies from 80 to 100 nm. We also observe the rough surface of the rGO which is full of wrinkles/folds. It is possible during spray-coating that thin rGO sheets may randomly cover AgNPs and they have the tendency to overlap one another. In fact, before reaching the surface, in solution, there is an interaction between sheets with each other at edge-to-edge contacts because of existence of activated functional groups at the edge of the GO sheet [9]. All above reasons lead to form wrinkles and folds after deposition of rGO. These wrinkles were believed to have variable height from 1.0 to 4.5 nm above the GO sheet. Herein, the XRD is used to confirm the formation of the HEL. In Figure 2(b), the feature diffraction peak (001) at 11.3° confirmed the structure of GO, corresponding to an interlayer d-spacing of 0.78 nm. This peak is shifted to 17.15° and becomes broader, indicating that the GO had been reduced to rGO. In case of AgNPs diffraction pattern, the peaks at 38.1°, 44.3°, 64.5°, and 77.5° could be referred to (111), (200), (220), and (311) crystallographic planes of the face centered cubic AgNPs, respectively, [JCPDS card No. 07-0783]. It is clear to see in Figure 2(b) that the XRD spectrum of the HEL is a combination of rGO and AgNPs diffraction pattern, which reconfirms the formation of HEL such as rGO covered AgNPs as shown in the SEM image (Figure 2(a)).

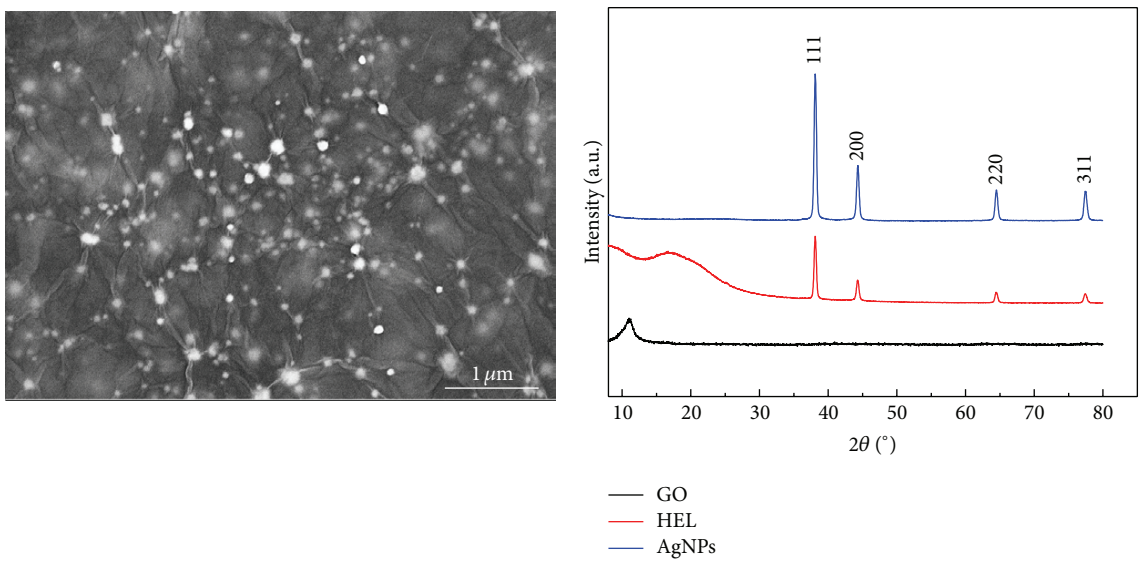

Figure 2: (a) Top-view SEM image of the HEL and (b) X-ray diffraction patterns of GO, HEL, and AgNPs film.

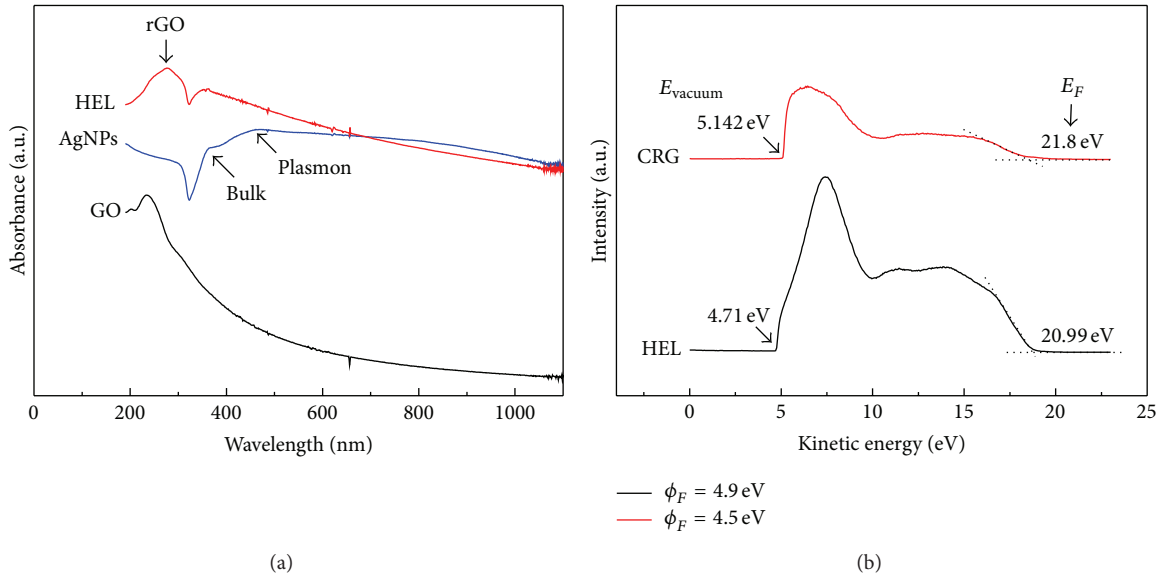

Figure 3: (a) UV-Vis spectra of CRG, HEL, and AgNPs. (b) UPS spectra of CRG and HEL.

Figure 3(a) represents the UV-Vis absorption spectra of the synthesized rGO, AgNPs, and HEL, respectively. For the GO sample, the observed absorption maximum at 233 nm is ascribed to $\pi \rightarrow \pi^*$ transition of aromatic C-C bonds, and the shoulder at 300 nm is attributed to $n \rightarrow \pi^*$ transition C=O bonds. In the case of AgNPs, the spectrum shows a broad plasmon peak at around 450 nm. It implies that the diameter of prepared AgNPs varied from 80 to 100 nm in accordance with the SEM results. Noguez reported that the absorption peak usually moves toward a longer wavelength when the particle increases in size [10]. A shoulder peak near 350 nm is attributed to the plasmon resonance of bulk silver. After the rGO is spray-coated on the AgNPs, a new peak appears at 264 nm which is referred to the conjugated C=C bonds of the rGO. It should be noted that the peak at 450 nm disappeared, and only bulk peak (350 nm) appeared after spray-coating of rGO onto AgNPs, suggesting that the rGO almost completely covered the AgNPs. The UV-Vis spectra are in good agreement with the SEM observations. Figure 3(b) shows the UPS spectra of reduced GO obtained by hydrazine reduction and as-synthesized HEL films. The work function (ϕ_F) was determined as $\phi_F = h\nu - (E_F - E_{vacuum})$, where $h\nu$ is the photon energy of excitation light (He I discharge lamp, 21.2 eV). The energy positions of the E_F are determined by linear extrapolation to the background where the spectrum ends. The work function of reduced GO

Table 1: Device parameters of PSCs with HEL (rGO/AgNPs/rGO), CRG, and Ref, respectively.

Device configuration	J_{SC} (mA/cm^2)	V_{OC} (V)	FF (%)	PCE (%)
(Ref): ITO/PDOT:PSS/P3HT:PCBM/Al	6.92	0.55	50	1.94
(HEL): ITO/HEL/PDOT:PSS/P3HT:PCBM/Al	7.27	0.55	51	2
(CRG): ITO/CRG/PDOT:PSS/P3HT:PCBM/Al	6.22	0.55	30	1.03

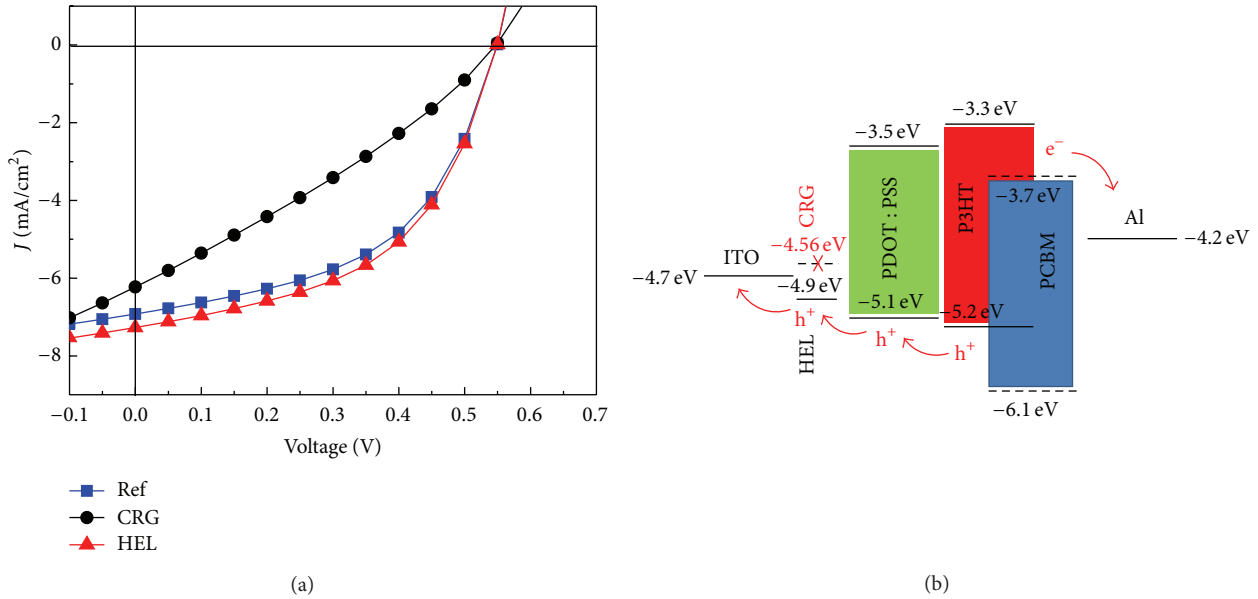

Figure 4: (a) *J-V* characteristics of the polymer solar cells with CRG and HEL as compared to reference. (b) The schematic band diagram of the polymer solar cells with HEL and CRG.

obtained by using hydrazine is estimated to be 4.5 eV, which is significantly higher than that of pristine graphene (4.2 eV) and smaller than that of GO (>5.0 eV). It is likely that the incorporation of electron withdrawing groups such as -OH to the surface of graphene increases the work function, whereas N-doping of rGO by hydrazine increases the electron density and thus decreases the work function as compared to GO. Our value is slightly higher than the reported experimental values within the range of 4.2–4.4 eV [11]. In case of HEL, the work function is found to be 4.9 eV, which is similar to the work function of graphene doped with AgNPs. Garg et al. demonstrated that the work function of graphene could be tuned from 4.3 eV to 5.0 eV by introducing Ag [12]. According to Figure 3(b), we have encountered that the work function of GO can be easily tuned to a value lower or higher than that of ITO by being reduced with hydrazine or sandwiched with AgNPs, respectively. To the best of our knowledge, as-synthesized sandwich structure rGO/AgNPs/rGO to regulate the work function of rGO has not been reported to date. This is a significant finding because it verified that rGO supported AgNPs acts as HEL for solar cells applications. Hence, it allows us to further examine the effect of synthesized HEL on polymer solar cells performance in the next part.

Figure 4(a) shows the *J-V* characteristics of the PSCs with two different types of inserted layer such as HEL (rGO/AgNPs/rGO) and CRG by using hydrazine reduction and without any inserted layer. The short circuit current density (J_{SC}), open-circuit voltage (V_{OC}), fill factor (FF), and power conversion efficiency (PCE) obtained from *J-V* curves are summarized in Table 1. The influence of the HEL work function on the device performance can be clearly observed. The J_{SC} of the device fabricated on HEL increases but decreases for the device fabricated on CRG in comparison to the reference device. The V_{OC} is found to be unchanged. Figure 4(b) illustrates the energy level diagram in order to explain the J_{SC}-dependence WF. The HEL with the WF higher than that of ITO is beneficial for extracting holes from active layer to ITO due to low interface barrier. In contrast, CRG with the WF lower than that of ITO is considered as a hole blocking layer. Therefore, a device with HEL is expected to show the highest efficiency. Nevertheless, slight enhancement of PCE was achieved as compared to reference device when HEL is incorporated. In fact, solution-based process of GO could not afford a smooth interface with active layer because large amount of functional groups remained on the GO surface [2]. Further optimization of reduction extent via the use of solution-processable should lead to additional development of the GO-based hole extraction layers in the device performance.

4. Conclusions

In conclusion, we report a solution-based process to fabricate a sandwiched structure of rGO/AgNPs/rGO acting as

an efficient HEL for PSCs device. The insertion of AgNPs between two layers of rGO allows us to manipulate the work function of rGO film. In order to investigate the effect of the work function on the PSCs device performance, a complementary device based on CRG in place of rGO/AgNPs/rGO was also created for comparison. Our results demonstrated that introducing rGO/AgNPs/rGO at the anode/active layer interface seems to be very favourable for the extraction of hole from active layer into ITO anode because of lowering of barrier level alignment at the interface. Consequently, sandwiched structure leads to significant improvement of J_{SC} and the overall photovoltaic performance.

Conflict of Interests

The authors declare that there is no conflict of interests regarding the publication of this paper.

Acknowledgments

This work was funded by Vietnam National University-Ho Chi Minh City (B2012-18-12TD) and Chonbuk National University in 2014. This research was also supported by Basic Science Research Program through the National Research Foundation of Korea (NRF) funded by the Ministry of Educaton (NRF-2014R1A1A2008104).

References

[1] S.-S. Li, K.-H. Tu, C.-C. Lin, C.-W. Chen, and M. Chhowalla, "Solution-processable graphene oxide as an efficient hole transport layer in polymer solar cells," *ACS Nano*, vol. 4, no. 6, pp. 3169–3174, 2010.

[2] J.-M. Yun, J.-S. Yeo, J. Kim et al., "Solution-processable reduced graphene oxide as a novel alternative to PEDOT:PSS hole transport layers for highly efficient and stable polymer solar cells," *Advanced Materials*, vol. 23, no. 42, pp. 4923–4928, 2011.

[3] J. Liu, M. Durstock, and L. Dai, "Graphene oxide derivatives as hole- and electron-extraction layers for high-performance polymer solar cells," *Energy & Environmental Science*, vol. 7, no. 4, pp. 1297–1306, 2014.

[4] H.-W. Tien, Y.-L. Huang, S.-Y. Yang, J.-Y. Wang, and C.-C. M. Ma, "The production of graphene nanosheets decorated with silver nanoparticles for use in transparent, conductive films," *Carbon*, vol. 49, no. 5, pp. 1550–1560, 2011.

[5] G.-Q. Fan, Q.-Q. Zhuo, J.-J. Zhu et al., "Plasmonic-enhanced polymer solar cells incorporating solution-processable Au nanoparticle-adhered graphene oxide," *Journal of Materials Chemistry*, vol. 22, no. 31, pp. 15614–15619, 2012.

[6] K. C. Kwon, W. J. Dong, G. H. Jung, J. Ham, J.-L. Lee, and S. Y. Kim, "Extension of stability in organic photovoltaic cells using UV/ozone-treated graphene sheets," *Solar Energy Materials and Solar Cells*, vol. 109, pp. 148–154, 2013.

[7] V. H. Pham, T. V. Cuong, S. H. Hur et al., "Fast and simple fabrication of a large transparent chemically-converted graphene film by spray-coating," *Carbon*, vol. 48, no. 7, pp. 1945–1951, 2010.

[8] T. V. Cuong, V. H. Pham, E. W. Shin et al., "Temperature-dependent photoluminescence from chemically and thermally reduced graphene oxide," *Applied Physics Letters*, vol. 99, no. 4, Article ID 041905, 2011.

[9] Y. Zhu, W. Cai, R. D. Piner, A. Velamakanni, and R. S. Ruoff, "Transparent self-assembled films of reduced graphene oxide platelets," *Applied Physics Letters*, vol. 95, no. 10, Article ID 103104, 2009.

[10] C. Noguez, "Surface plasmons on metal nanoparticles: the influence of shape and physical environment," *The Journal of Physical Chemistry C*, vol. 111, no. 10, pp. 3606–3619, 2007.

[11] J. O. Hwang, J. S. Park, D. S. Choi et al., "Workfunction-tunable, N-doped reduced graphene transparent electrodes for high-performance polymer light-emitting diodes," *ACS Nano*, vol. 6, no. 1, pp. 159–167, 2012.

[12] R. Garg, N. Dutta, and N. Choudhury, "Work function engineering of graphene," *Nanomaterials*, vol. 4, no. 2, pp. 267–300, 2014.